

Impact of the LZ Experiment on DM Phenomenology and Naturalness in the MSSM

Li Dongwei¹, Meng Lei², and Zhou Haijing^{2*}

¹*Fundamentals Department, Henan Police College, Zhengzhou 450046, China*

²*School of Physics, Henan Normal University, Henan Xinxiang 453007, China*

Abstract

Taking the bino-dominated dark matter (DM) as an example, through approximate analytical formulas and numerical results, this paper analyzes the impact of the LUX-ZEPLIN (LZ) experiment on the DM phenomenology and naturalness in the Minimal Supersymmetric Standard Model (MSSM). The conclusion is that the limitation of the latest LZ experiment worsens the naturalness of the MSSM. This phenomenon manifests itself in the predictions of the Z -boson mass and dark matter relic density, particularly the Z - and h -mediated resonant annihilations.

*Email: zhouhaijing0622@163.com

1 Introduction

Supersymmetric models of particle physics are renowned for providing an elegant solution to the daunting gauge hierarchy problem. As the most economical supersymmetric expansion model, the Minimal Supersymmetric Standard Model (MSSM) may provide a solid description of nature from the weak scale to energy scales associated with the grand unification[1], which also receives indirect experimental support from the measured strengths of weak-scale gauge couplings, measured value of the top quark mass, and discovery of a SM Higgs-like boson by Atlas[2] and CMS[3] in 2012. However, this audacious extrapolation has suffered a string of serious set-backs: no signs of supersymmetric matter have emerged from LHC data or DM data, which has led some physicists to call into question whether weak-scale SUSY really exists or at least to concede that it suffers diversiform unattractive fine tunings [4].

In the MSSM, the Z-boson mass is given by [5]

$$\frac{m_Z^2}{2} = \frac{m_{H_d}^2 + \Sigma_d^d - (m_{H_u}^2 + \Sigma_u^u) \tan^2 \beta}{\tan^2 \beta - 1} - \mu^2, \quad (1)$$

where $m_{H_u}^2$ and $m_{H_d}^2$ are soft SUSY-breaking (not physical) Higgs mass terms, μ is the superpotential Higgsino mass term, $\tan \beta \equiv v_u/v_d$ is the ratio of Higgs field vevs, and Σ_u^u and Σ_d^d include various independent radiative corrections[6]. Since the $(m_{H_d}^2 + \Sigma_d^d)$ term is suppressed by $\tan^2 \beta - 1$, for even moderate $\tan \beta$ values, Eq. (1) approximately reduces to

$$\frac{m_Z^2}{2} \simeq -(m_{H_u}^2 + \Sigma_u^u) - \mu^2. \quad (2)$$

To naturally achieve $m_Z \simeq 91.2$ GeV, $-m_{H_u}^2$, $-\mu^2$, and each contribution to $-\Sigma_u^u$ should be comparable in magnitude to $m_Z^2/2$. The extent of the comparability can be quantified using the electroweak fine-tuning parameter[7]

$$\Delta_{EW} \equiv \max_i |C_i| / (M_Z^2/2), \quad (3)$$

where $C_{H_u} = -m_{H_u}^2$, $C_\mu = -\mu^2$, and $C_{\Sigma_u^u} = \Sigma_u^u$. A low value of Δ_{EW} means less fine tuning, and $1/\Delta_{EW}$ is the percentage of fine tuning., *e.g.*, $\Delta_{EW} = 20$ corresponds to $\Delta_{EW}^{-1} = 5\%$ fine tuning among the terms that contribute to $m_Z^2/2$. Therefore, given the experimental lower bound, there is general agreement that smaller values of $|\mu|$ are preferred in fine-tuning issues. However, the current experiment limits have imposed a strong lower bound on $|\mu|$. For example, in 2017, the analysis of a global fit for the MSSM, which considered various experimental constraints¹ showed that $\mu > 350$ GeV was favored at a 95% confidence level[8]. This value of μ can induce a tuning of approximately 3% to predict the Z-boson mass. The studies in Ref. [12] showed that the Xenon-1T direct search limits[13] imposed a strong lower bound on $|\mu|$, in particular for $\mu > 0$ or if the masses of the heavy Higgs bosons of the MSSM are near their current limit from LHC searches. The studies in Ref. [14] showed that μ should be larger than approximately 500 GeV for $M_1 < 0$ and 630 GeV for $M_1 > 100$ GeV after considering the recent measurement

¹These experimental constraints include those from the DM relic density, PandaX-II (2017) results for the SI cross section [9], PICO results for the SD cross section[10], and the searches for supersymmetric particles at the 13-TeV LHC with $36fb^{-1}$ data (especially the CMS analysis of the electroweakino production) [11].

of the muon anomalous magnetic moment at Fermilab [15], recently released first results of the LUX-ZEPLIN (LZ) experiment in the direct search for DM [16], and rapid progress of the LHC search for supersymmetry[11, 17, 18]. These improved bounds imply a tuning of $\mathcal{O}(1\%)$ to predict the Z -boson mass.

In this paper, through approximate analytical formulas and numerical results, we analyzed in detail the DM phenomenology and the associated unnaturalness in the MSSM under the latest LZ experimental limits. The remainder of this paper is organized as follows. In section 2, we briefly introduce the neutralino sections of the MSSM and demonstrate DM scattering cross-sections with nucleons and annihilation for bino-like $\tilde{\chi}_1^0$ using the approximate analytical formulas. In section 3, we briefly describe our scanning strategy and investigate the predictions for surviving samples and properties of bino-dominated DM scenarios to understand the associated unnaturalness. We reserve section 4 for our conclusions.

2 Dark Matter Section in the MSSM

In the MSSM, the neutralino mass matrix in the basis of $\Psi^0 = (-i\tilde{B}^0, -i\tilde{W}^0, \tilde{H}_d^0, \tilde{H}_u^0)$ is given by[19]:

$$M_{\text{neut}} = \begin{pmatrix} M_1 & 0 & -c_\beta s_W m_Z & s_\beta s_W m_Z \\ 0 & M_2 & c_\beta c_W m_Z & -s_\beta c_W m_Z \\ -c_\beta s_W m_Z & c_\beta c_W m_Z & 0 & -\mu \\ s_\beta s_W m_Z & -s_\beta c_W m_Z & -\mu & 0 \end{pmatrix}, \quad (4)$$

where M_1 , M_2 , and μ are the soft SUSY-breaking mass parameters of the Bino, Wino, and Higgsinos, respectively. m_Z is the Z -boson mass, θ_w is the Weinberg angle ($c_W \equiv \cos \theta_W$ and $s_W \equiv \sin \theta_W$), $\tan \beta \equiv s_\beta/c_\beta = v_u/v_d$ is the ratio of the vacuum expectation values for the two Higgs doublets ($c_\beta \equiv \cos \beta$ and $s_\beta \equiv \sin \beta$), and $v^2 = v_u^2 + v_d^2 = (246\text{GeV})^2$. Diagonalizing M_{neut} with a unitary matrix N of 4×4 yields the masses of the physical states $\tilde{\chi}_i^0$ (ordered by mass) of the four neutralinos:

$$N^* M_{\text{neut}} N^{-1} = \text{diag}\{m_{\chi_1^0}, m_{\chi_2^0}, m_{\chi_3^0}, m_{\chi_4^0}\}$$

with

$$\tilde{\chi}_i^0 = N_{i1}\tilde{B}^0 + N_{i2}\tilde{W}^0 + N_{i3}\tilde{H}_d^0 + N_{i4}\tilde{H}_u^0 \quad (i = 1, 2, 3, 4),$$

where m_{χ_i} are the roots to the following eigenequation:

$$(x - M_1)(x - M_2)(x^2 - \mu^2) - m_Z^2(x - M_1 c_W^2 - M_2 s_W^2)(2\mu s_\beta c_\beta + x) = 0, \quad (5)$$

and the eigenvectors of m_{χ_i} is the column vector constituted by $N_{ij}(j = 1, 2, 3, 4)$, which is given by

$$N_i = \frac{1}{\sqrt{C_i}} \begin{pmatrix} (\mu^2 - m_{\tilde{\chi}_i^0}^2)(M_2 - m_{\tilde{\chi}_i^0})s_W \\ -(\mu^2 - m_{\tilde{\chi}_i^0}^2)(M_1 - m_{\tilde{\chi}_i^0})c_W \\ (M_2 s_W^2 + M_1 c_W^2 - m_{\tilde{\chi}_i^0}^2)(m_{\tilde{\chi}_i^0} c_\beta + \mu s_\beta)m_Z \\ -(M_2 s_W^2 + M_1 c_W^2 - m_{\tilde{\chi}_i^0}^2)(m_{\tilde{\chi}_i^0} s_\beta + \mu c_\beta)m_Z \end{pmatrix}. \quad (6)$$

The specific form of the normalization factor C_i is as follows:

$$C_i = (\mu^2 - m_{\tilde{\chi}_i^0}^2)^2 (M_2 - m_{\tilde{\chi}_i^0})^2 s_W^2 + (\mu^2 - m_{\tilde{\chi}_i^0}^2)^2 (M_1 - m_{\tilde{\chi}_i^0})^2 c_W^2 + (M_2 s_W^2 + M_1 c_W^2 - m_{\tilde{\chi}_i^0})^2 (\mu^2 + m_{\tilde{\chi}_i^0}^2 + 2\mu m_{\tilde{\chi}_i^0} s_\beta c_\beta) m_Z^2. \quad (7)$$

Then, the diagonalizing matrix is $N = \{N_1, N_2, N_3, N_4\}$, where $i = 1, 2, 3, 4$ correspond to the bino, wino, higgsino-down, and higgsino-up components, respectively.

The lightest neutralino, $\tilde{\chi}_1^0$, which acts as the DM candidate, is the focus of this work. N_{11}^2 , N_{12}^2 , and $N_{13}^2 + N_{14}^2$ are the bino, wino, and higgsino components in the physical state $\tilde{\chi}_1^0$, respectively, and satisfy $N_{11}^2 + N_{12}^2 + N_{13}^2 + N_{14}^2 = 1$. We call $\tilde{\chi}_1^0$ the bino-dominant DM (wino- or higgsino-) if $N_{11}^2 > 0.5$ ($N_{12}^2 > 0.5$ or $N_{13}^2 + N_{14}^2 > 0.5$). The couplings of DM to the scalar Higgs states and Z-boson are included in the calculation of DM-nucleon cross sections and DM annihilation, which correspond to the Lagrangian[20, 21]:

$$\mathcal{L}_{MSSM} \ni C_{\tilde{\chi}_1^0 \tilde{\chi}_1^0 h} h \tilde{\chi}_1^0 \tilde{\chi}_1^0 + C_{\tilde{\chi}_1^0 \tilde{\chi}_1^0 H} H \tilde{\chi}_1^0 \tilde{\chi}_1^0 + C_{\tilde{\chi}_1^0 \tilde{\chi}_1^0 Z} Z_\mu \tilde{\chi}_1^0 \gamma^\mu \gamma_5 \tilde{\chi}_1^0,$$

and the coefficients are given by

$$C_{\tilde{\chi}_1^0 \tilde{\chi}_1^0 h} \approx \frac{2m_Z^2 \mu}{v C_1} (\mu^2 - m_{\tilde{\chi}_1^0}^2) (M_2 s_W^2 + M_1 c_W^2 - m_{\tilde{\chi}_1^0})^2 \left(\frac{m_{\tilde{\chi}_1^0}}{\mu} + \sin 2\beta \right), \quad (8)$$

$$C_{\tilde{\chi}_1^0 \tilde{\chi}_1^0 H} \approx \frac{2m_Z^2 \mu}{v C_1} (\mu^2 - m_{\tilde{\chi}_1^0}^2) (M_2 s_W^2 + M_1 c_W^2 - m_{\tilde{\chi}_1^0})^2 \cos 2\beta, \quad (9)$$

$$C_{\tilde{\chi}_1^0 \tilde{\chi}_1^0 Z} \approx \frac{m_Z^3}{v C_1} (\mu^2 - m_{\tilde{\chi}_1^0}^2) (M_2 s_W^2 + M_1 c_W^2 - m_{\tilde{\chi}_1^0})^2 \cos 2\beta, \quad (10)$$

where h and H are two CP-even Higgs states predicted by the MSSM: the SM-like Higgs boson and non-SM doublet Higgs boson, respectively.

Serving as a weakly interacting massive particle (WIMP), $\tilde{\chi}_1^0$ may be detected by measuring their spin-independent (SI) and spin-dependent (SD) scattering cross-sections after an elastic scattering of $\tilde{\chi}_1^0$ on a nucleus has occurred. At the tree level, the contribution to the SD (SI) scattering cross-section in the heavy squark limit is dominated by the t-channel Z-boson (CP-even Higgs bosons h_i) exchange diagram. Therefore, the scattering cross-sections take the following form [14, 22, 23]:

$$\sigma_{\tilde{\chi}_1^0-N}^{SD} \approx C_N \times \left(\frac{C_{\tilde{\chi}_1^0 \tilde{\chi}_1^0 Z}}{0.01} \right)^2, \quad (11)$$

$$\begin{aligned} \sigma_{\tilde{\chi}_1^0-N}^{SI} &= \frac{m_N^2}{\pi v^2} \left(\frac{m_N m_{\tilde{\chi}_1^0}}{m_N + m_{\tilde{\chi}_1^0}} \right)^2 \left(\frac{1}{125 \text{ GeV}} \right)^4 \times \\ &\quad \left\{ (F_u^N + F_d^N) C_{\tilde{\chi}_1^0 \tilde{\chi}_1^0 h} \left(\frac{125 \text{ GeV}}{m_h} \right)^2 + \left(\frac{F_u^N}{\tan \beta} - F_d^N \tan \beta \right) C_{\tilde{\chi}_1^0 \tilde{\chi}_1^0 H} \left(\frac{125 \text{ GeV}}{m_H} \right)^2 \right\}^2 \\ &\approx 6.4 \times 10^{-44} \text{ cm}^2 \times \left(\frac{F_u^N + F_d^N}{0.28} \right)^2 \times \\ &\quad \left\{ \left(\frac{F_u^N}{F_u^N + F_d^N} \right) \times \left[\frac{C_{\tilde{\chi}_1^0 \tilde{\chi}_1^0 h}}{0.1} \left(\frac{125 \text{ GeV}}{m_h} \right)^2 + \frac{1}{\tan \beta} \frac{C_{\tilde{\chi}_1^0 \tilde{\chi}_1^0 H}}{0.1} \left(\frac{125 \text{ GeV}}{m_H} \right)^2 \right] \right. \\ &\quad \left. + \left(\frac{F_d^N}{F_u^N + F_d^N} \right) \times \left[\frac{C_{\tilde{\chi}_1^0 \tilde{\chi}_1^0 h}}{0.1} \left(\frac{125 \text{ GeV}}{m_h} \right)^2 - \tan \beta \frac{C_{\tilde{\chi}_1^0 \tilde{\chi}_1^0 H}}{0.1} \left(\frac{125 \text{ GeV}}{m_H} \right)^2 \right] \right\}^2, \quad (12) \end{aligned}$$

where $N=p$, n represents the proton and neutron, and $C_p \simeq 2.9 \times 10^{-41} \text{ cm}^2$ ($C_n \simeq 2.3 \times 10^{-41} \text{ cm}^2$) [24, 25]. The form factors (at zero momentum transfer) are $F_d^{(N)} = f_d^{(N)} + f_s^{(N)} + \frac{2}{27}f_G^{(N)}$ and $F_u^{(N)} = f_u^{(N)} + \frac{4}{27}f_G^{(N)}$, where $f_q^{(N)} = m_N^{-1} \langle N | m_q q \bar{q} | N \rangle$ ($q = u, d, s$) is the normalized light quark contribution to the nucleon mass, and $f_G^{(N)} = 1 - \sum_{q=u,d,s} f_q^{(N)}$ affects other heavy quark mass fractions in the nucleons [26, 27]. In this study, the default settings for $f_q^{(N)}$ were used in the micrOMEGAs package [28], and they predict $F_u^p \simeq F_u^n \simeq 0.15$ and $F_d^p \simeq F_d^n \simeq 0.13$. Hence, the DM-proton scattering and DM-neutron scattering have approximately equal SI cross-sections (i.e., $\sigma_{\tilde{\chi}_1^0-p}^{SI} \simeq \sigma_{\tilde{\chi}_1^0-n}^{SI}$) [29].

In the pure bino limit ($m_{\tilde{\chi}_1^0} \approx M_1$ and $N_{11}^2 \approx 1$), the above formulas can be approximated as

$$C_1 = (\mu^2 - m_{\tilde{\chi}_1^0}^2)(m_{\tilde{\chi}_1^0} - M_2)^2 s_W^2, \quad (13)$$

$$C_{\tilde{\chi}_1^0 \tilde{\chi}_1^0 h} \approx \frac{2m_Z^2 \mu s_W^2}{v(\mu^2 - m_{\tilde{\chi}_1^0}^2)} \left(\frac{m_{\tilde{\chi}_1^0}}{\mu} + \sin 2\beta \right), \quad (14)$$

$$C_{\tilde{\chi}_1^0 \tilde{\chi}_1^0 H} \approx \frac{2m_Z^2 \mu s_W^2}{v(\mu^2 - m_{\tilde{\chi}_1^0}^2)} \cos 2\beta, \quad (15)$$

$$C_{\tilde{\chi}_1^0 \tilde{\chi}_1^0 Z} \approx \frac{m_Z^3 s_W^2}{v(\mu^2 - m_{\tilde{\chi}_1^0}^2)} \cos 2\beta. \quad (16)$$

Meanwhile, taking $F_d^{(N)} \simeq F_u^{(N)} \simeq 0.14$ [30] and $\tan \beta \gg 1$, one can conclude that

$$\sigma_{\tilde{\chi}_1^0-n}^{SD} \approx 2.4 \times 10^{-40} \text{ cm}^2 \times \frac{m_Z^2 v^2}{\mu^4} \times \left(\frac{1}{1 - m_{\tilde{\chi}_1^0}^2/\mu^2} \right)^2, \quad (17)$$

$$\begin{aligned} \sigma_{\tilde{\chi}_1^0-N}^{SI} &\approx 2.1 \times 10^{-45} \text{ cm}^2 \times \frac{v^2}{\mu^2} \times \left(\frac{1}{1 - m_{\tilde{\chi}_1^0}^2/\mu^2} \right)^2 \\ &\times \left\{ \left(\frac{m_{\tilde{\chi}_1^0}}{\mu} + \sin 2\beta \right) \left(\frac{125 \text{ GeV}}{m_h} \right)^2 + \frac{\tan \beta}{2} \left(\frac{125 \text{ GeV}}{m_H} \right)^2 \right\}^2. \end{aligned} \quad (18)$$

The two analytic formulas suggest that σ^{SD} and σ^{SI} are suppressed by μ^4 and μ^2 , respectively. Moreover, if $(\frac{m_{\tilde{\chi}_1^0}}{\mu} + \sin 2\beta)$ and $\tan \beta$ have opposite signs, the contributions to σ^{SI} from the light (h) and heavy (H) Higgs exchange channels destructively interfere with each other. σ^{SI} will vanish for $(\frac{m_{\tilde{\chi}_1^0}}{\mu} + \sin 2\beta) \left(\frac{1}{m_h} \right)^2 + \frac{\tan \beta}{2} \left(\frac{1}{m_H} \right)^2 \rightarrow 0$, which is known as the ‘‘generalized blind spot’’ [23, 30]. For the convenience of subsequent descriptions, we define $\mathcal{A}_h = (\frac{m_{\tilde{\chi}_1^0}}{\mu} + \sin 2\beta) \left(\frac{125 \text{ GeV}}{m_h} \right)^2$ and $\mathcal{A}_H = \frac{\tan \beta}{2} \left(\frac{125 \text{ GeV}}{m_H} \right)^2$ to represent the contributions from h and H to the SI cross section, respectively.

For DM produced via the standard thermal freeze-out, the relic density at freeze-out temperature $T_F \equiv m_{\tilde{\chi}_1^0}/x_F$ (typically, $x_F \simeq 20$) is approximately [23]

$$\Omega_{\tilde{\chi}_1^0} h^2 \sim 0.12 \times \frac{2.5 \times 10^{-26} \text{ cm}^3/\text{s}}{\langle \sigma v \rangle_{x_F}}, \quad (19)$$

where $\langle\sigma v\rangle_{x_F}$ corresponds to the effective (thermally averaged) annihilation cross section. To match the observed DM relic density ($\Omega_{\text{DM}}h^2 \simeq 0.12$) [31], it is required that $\langle\sigma v\rangle_{x_F} \sim 2.5 \times 10^{-26} \text{cm}^3/\text{s}$.

In the MSSM, for $m_{\tilde{\chi}_1^0} < 1\text{TeV}$, only the bino-dominated $\tilde{\chi}_1^0$ can predict the correct DM relic density, and the interactions of the higgsino- or wino-dominated $\tilde{\chi}_1^0$ with the Standard Model particles are relatively strong so that the predicted relic density is much smaller than the observed DM relic density[32]. In our scenario, taking the example of the bino-like $\tilde{\chi}_1^0$, the fine tunings introduced by the DM sector in the MSSM under the current DM experimental limits will be discussed. For bino-like $\tilde{\chi}_1^0$, the contributions to $\langle\sigma v\rangle_{x_F}$ are from two channels

- The Z- or h-mediated resonant annihilation [33, 34]. The corresponding annihilation cross sections are approximated to [35]

$$\langle\sigma v\rangle_{x_F}^{d\bar{d},Z} \sim (2.5 \times 10^{-26} \frac{\text{cm}^3}{\text{s}}) \times \left[\left(\frac{0.46m_d}{1\text{GeV}} \right) \times \frac{C_{\tilde{\chi}_1^0\tilde{\chi}_1^0 Z}}{\left(1 - \frac{m_Z^2}{4m_{\tilde{\chi}_1^0}^2}\right)} \right]^2 \left(\frac{m_{\tilde{\chi}_1^0}}{46\text{GeV}} \right)^{-4}, \quad (20)$$

$$\langle\sigma v\rangle_{x_F}^{d\bar{d},h} \sim (2.5 \times 10^{-26} \frac{\text{cm}^3}{\text{s}}) \times \left[\left(\frac{0.048m_d}{1\text{GeV}} \right) \times \frac{C_{\tilde{\chi}_1^0\tilde{\chi}_1^0 h}}{\left(1 - \frac{m_h^2}{4m_{\tilde{\chi}_1^0}^2}\right)} \right]^2 \left(\frac{m_{\tilde{\chi}_1^0}}{62\text{GeV}} \right)^{-2}. \quad (21)$$

Due to the hierarchy of the Yukawa couplings, the contribution to the thermal cross section from ($\tilde{\chi}_1^0\tilde{\chi}_1^0 \rightarrow q\bar{q}$) annihilations will be dominated by the bottom quarks for lighter $m_{\tilde{\chi}_1^0}$. Here, m_d is the down-type quark mass. As shown in the expression, the measured relic density requires a high degeneracy between $m_{Z(h)}$ and $2m_{\tilde{\chi}_1^0}$. We define degeneracy parameters $\Delta_{Z(h)} = \left|1 - \frac{m_{Z(h)}^2}{4m_{\tilde{\chi}_1^0}^2}\right|$ to quantize the fine tuning between $m_{Z(h)}$ and $2m_{\tilde{\chi}_1^0}$, e.g., $\Delta_Z = 10^{-3}$ implies 0.1% fine tuning among m_Z and $2m_{\tilde{\chi}_1^0}$,

- The co-annihilation with sleptons, wino-dominated neutralinos, and/or charginos [14, 23, 33, 34, 37, 38, 39, 40, 41]. The corresponding reactions are $\tilde{\chi}_i\tilde{\chi}_j \rightarrow XX'$, where X and X' donate SM particles. In the case, $\langle\sigma v\rangle_{x_F}$ in Eq. (19) should be replaced by $\langle\sigma_{eff}v\rangle_{x_F}$, where σ_{eff} is given by [36]

$$\sigma_{eff} = \sum_{i,j} \sigma_{ij} \frac{g_i g_j}{g_{eff}} (1 + \Delta_i)^{3/2} (1 + \Delta_j)^{3/2} \times \exp[-x(\Delta_i + \Delta_j)], \quad (22)$$

where

$$\sigma_{ij} = \sigma(\tilde{\chi}_i\tilde{\chi}_j \rightarrow XX'),$$

$$g_{eff} \equiv \sum_i g_i (1 + \Delta_i)^{3/2} \exp(-x\Delta_i),$$

$$\Delta_i \equiv (m_i - m_{\tilde{\chi}_1^0})/m_{\tilde{\chi}_1^0},$$

$x \equiv m_{\tilde{\chi}_1^0}/T$. g_i represents the internal degrees of freedom, and Δ_i parameterizes the mass splitting. In the co-annihilation case, the right relic abundance usually requires holding Δ_i at the 5 – 15% level[36], which also corresponds to one fine tuning.

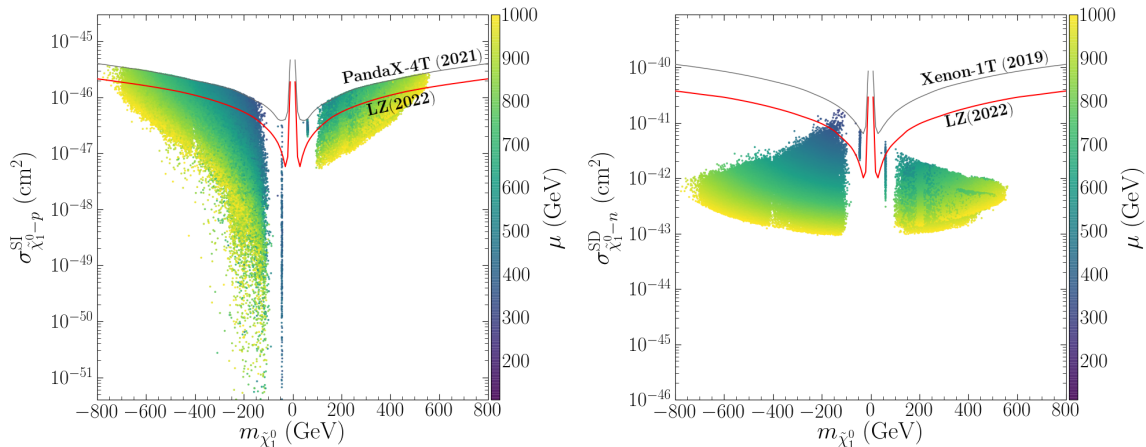


Figure 1: Projection of the obtained samples onto $m_{\tilde{\chi}_1^0} - \sigma_{\tilde{\chi}_1^0-p}^{SI}$ (left panel) and $m_{\tilde{\chi}_1^0} - \sigma_{\tilde{\chi}_1^0-n}^{SD}$ (right panel). The colors indicate the value of the Higgsino mass μ .

3 Numerical Results and Theoretical Analysis

We employed the MultiNest algorithm [42] with $n_{\text{live}} = 10000^2$ to comprehensively scan the following parameter space:

$$\begin{aligned} 1 \leq \tan \beta \leq 60, \quad 0.1 \text{ TeV} \leq \mu \leq 1 \text{ TeV}, \quad 0.5 \text{ TeV} \leq M_A \leq 10 \text{ TeV}, \\ -1.0 \text{ TeV} \leq M_1 \leq 1.0 \text{ TeV}, \quad 0.1 \text{ TeV} \leq M_2 \leq 1.5 \text{ TeV}, \\ -5 \text{ TeV} \leq A_t = A_b \leq 5 \text{ TeV}, \quad 0.1 \text{ TeV} \leq M_{\tilde{\mu}_L}, M_{\tilde{\mu}_R} \leq 1 \text{ TeV}, \end{aligned}$$

where $\tan \beta$ is defined at the electroweak scale, and the others are defined at the renormalization scale $Q = 1 \text{ TeV}$. To obtain the SM-like Higgs boson mass ($m_h \approx 125 \text{ GeV}$), the soft trilinear coefficients A_t and A_b are assumed to be equal and freely change to adjust the Higgs mass spectrum. The second-generation sleptons ($M_{\tilde{\mu}_L}, M_{\tilde{\mu}_R}$) are used as free parameters to predict the measured DM relic abundance by co-annihilation with sleptons. Other unimportant parameters are fixed at 3 TeV, which include the gluino mass M_3 , SUSY parameters of the first- and third-generation sleptons, and three generations of squarks except A_t and A_b . During the scan, the likelihood function to guide the process considers the experimental constraints, including the consistency of h 's properties with the LHC Higgs data at the 95% confidence level (C.L.) [43], collider searches for extra Higgs bosons [44], $\pm 10\%$ at approximately the central value of the DM relic density from the Planck-2018 data [31], 90% C.L. upper bounds of the

²The n_{live} parameter in the algorithm controls the number of active points sampled in each iteration of the scan.

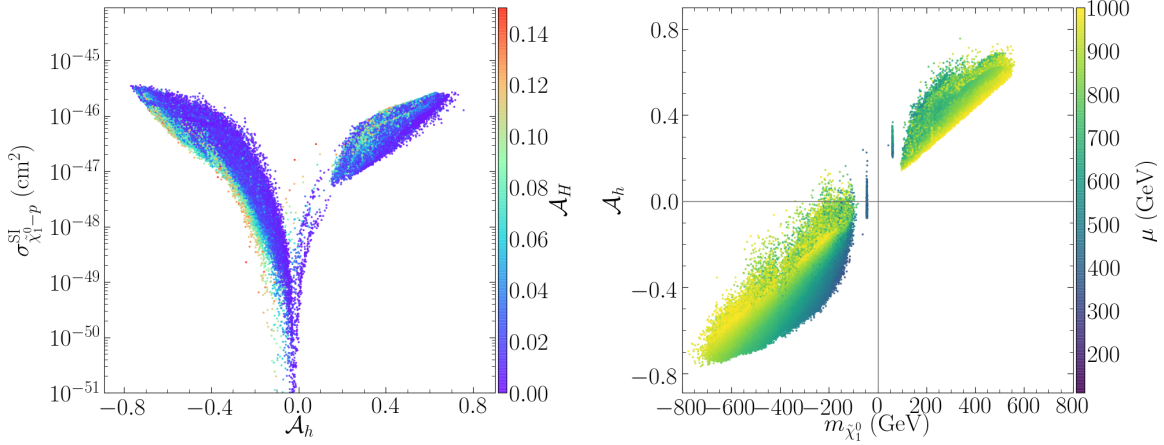


Figure 2: Projection of the surviving samples onto the $\mathcal{A}_h - \sigma_{\tilde{\chi}_1^0-p}^{SI}$ plane, where the colors indicate the contributions from H to the SI cross section \mathcal{A}_H , and onto the $m_{\tilde{\chi}_1^0} - \mathcal{A}_h$ plane, where the colors indicate the value of the Higgsino mass μ .

PandaX-4T experiment on the SI DM-nucleon scattering [45] and XENON-1T experiment on the SD scattering [46], 2σ bounds on the branching ratios of $B \rightarrow X_s \gamma$ and $B_s \rightarrow \mu^+ \mu^-$ [47], and vacuum stability of the scalar potential, which consists of the Higgs fields and the last two generations of the slepton fields [48, 49].

In Fig. 1, we project the surviving samples on the $m_{\tilde{\chi}_1^0} - \sigma_{\tilde{\chi}_1^0-p}^{SI}$ plane and $m_{\tilde{\chi}_1^0} - \sigma_{\tilde{\chi}_1^0-n}^{SD}$ plane, where the colors indicate the value of the Higgsino mass μ . Fig. 1 shows that $\sigma_{\tilde{\chi}_1^0-n}^{SD}$ is only related to μ and will be suppressed by a large μ , which is consistent with the analysis based on Eq. (17), i.e., $\sigma_{\tilde{\chi}_1^0-n}^{SD}$ is proportional to $\frac{m_Z^2 v^2}{\mu^4}$. The current LZ experiment constraint on $\sigma_{\tilde{\chi}_1^0-n}^{SD}$ requires that μ is greater than 370 GeV. However, the distribution of $\sigma_{\tilde{\chi}_1^0-p}^{SI}$ values is relatively complex. Although large μ can suppress $\sigma_{\tilde{\chi}_1^0-p}^{SI}$, $\sigma_{\tilde{\chi}_1^0-p}^{SI}$ can also be small for small μ . Based on Eq. (18), $\sigma_{\tilde{\chi}_1^0-p}^{SI}$ should be related to a combination of M_1 , μ , $\tan \beta$, and m_H . To find the combination that will make $\sigma_{\tilde{\chi}_1^0-p}^{SI}$ satisfy the latest experimental limit, as presented in Fig. 2, we projected the surviving samples onto the $\mathcal{A}_h - \sigma_{\tilde{\chi}_1^0-p}^{SI}$ plane, where the colors indicate the contributions from H to the SI cross section \mathcal{A}_H , and onto the $m_{\tilde{\chi}_1^0} - \mathcal{A}_h$ plane, where the colors indicate the value of the Higgsino mass μ . The contribution of the Heavy Higgs (H) to the SI cross-section for most samples is suppressed below 0.14 by m_H . Fig. 2 shows that compared with the contributions from H (\mathcal{A}_H) and v^2/μ^2 to the SI cross section, the contribution of h (\mathcal{A}_h) plays a dominant role. Next, we divided the samples into the following three categories to discuss in detail.

1. Type-I samples: $m_{\tilde{\chi}_1^0} \approx -\frac{1}{2}m_Z$, $5 < \tan \beta < 58$, $337\text{GeV} < \mu < 462\text{GeV}$, $100\text{GeV} < M_2 < 1206\text{GeV}$. $\tilde{\chi}_1^0$ is mainly annihilated to $d\bar{d}$ by exchanging a resonant Z-boson in the s-channel to obtain its measured relic density. According to Eq. (20), the corresponding

annihilation cross section in this area is approximately

$$\langle\sigma v\rangle_{x_F}^{d\bar{d},Z} \simeq (2.5 \times 10^{-26} \frac{\text{cm}^3}{\text{s}}) \left[\frac{2.2 \times 10^{-3} \times C_{\tilde{\chi}_1^0 \tilde{\chi}_1^0 Z}}{\Delta_Z} \right]^2 \left(\frac{m_{\tilde{\chi}_1^0}}{46 \text{GeV}} \right)^{-4}. \quad (23)$$

In the case, from Fig. 1, $\sigma_{\tilde{\chi}_1^0-p}^{SI}$ can also satisfy the direct detection constraints with small values of μ , but $\sigma_{\tilde{\chi}_1^0-n}^{SD}$ cannot. As discussed above, $\sigma_{\tilde{\chi}_1^0-p}^{SI}$ is proportional to $(\mathcal{A}_h + \mathcal{A}_H)$ in addition to being suppressed by μ^2 , and it even vanishes under the limits of M_1 , μ , $\tan\beta$, and m_H being arranged. Fig. 2 shows that $|\mathcal{A}_h| < 0.1$, which corresponds to M_1/μ and $\tan\beta$ having opposite signs, suppresses the SI cross section. However, $\sigma_{\tilde{\chi}_1^0-n}^{SD}$ is only proportional to $\frac{m_Z^2 v^2}{\mu^4}$. According to Eq. (17), the LZ direct detection constraints on the SD cross section requires $\mu > 500 \text{GeV}$ for these samples, which corresponds to $\Delta_{EW}^{-1} = 1.7\%$. According to Eqs. (16) and (23), $\mu = 500 \text{GeV}$ corresponds to $C_{\tilde{\chi}_1^0 \tilde{\chi}_1^0 Z} = 3 \times 10^{-3}$, i.e., to predict the correct relic density, $\Delta_Z = 6.6 \times 10^{-6}$, which implies a tuning of $\mathcal{O}(0.0001\%)$. A larger μ corresponds to a more severe fine tuning, so μ cannot be very large in this case.

2. Type-II samples: $m_{\tilde{\chi}_1^0} \simeq \frac{1}{2} m_h$, $7 < \tan\beta < 33$, $406 \text{GeV} < \mu < 776 \text{GeV}$, $100 \text{GeV} < M_2 < 994 \text{GeV}$. $\tilde{\chi}_1^0$ is mainly annihilated to $b\bar{b}$ through the s-channel exchange of a resonant SM-like Higgs boson h to obtain its measured relic density. According to Eq. (21), the corresponding annihilation cross section is approximated to

$$\langle\sigma v\rangle_{x_F}^{b\bar{b},h} \simeq (2.5 \times 10^{-26} \frac{\text{cm}^3}{\text{s}}) \left[\frac{0.2 \times C_{\tilde{\chi}_1^0 \tilde{\chi}_1^0 h}}{\Delta_h} \right]^2 \left(\frac{m_{\tilde{\chi}_1^0}}{62 \text{GeV}} \right)^2. \quad (24)$$

Compared with the Type-I samples, the μ value increases in the case. For most samples, $\mu > 500 \text{GeV}$ so that $\sigma_{\tilde{\chi}_1^0-n}^{SD}$ can satisfy the direct detection constraints, but $\sigma_{\tilde{\chi}_1^0-p}^{SI}$ cannot. From Fig. 2, the range of \mathcal{A}_h is (0.2,0.37), and the elevating effect of $(\mathcal{A}_h + \mathcal{A}_H)$ on $\sigma_{\tilde{\chi}_1^0-p}^{SI}$ has an advantage over the suppressing effect of μ^2 . At this time, M_1/μ and $\tan\beta$ have identical signs. For $\tan\beta = 10(30)$, according to Eq. (18), the direct detection constraints on the SI cross section increase μ to above 1500GeV (1200GeV), which corresponds to $\Delta_{EW}^{-1} = 0.2\%(0.3\%)$. According to Eq. (14), for $\mu = 1500 \text{GeV}(1200 \text{GeV})$, $C_{\tilde{\chi}_1^0 \tilde{\chi}_1^0 h} = 3(4) \times 10^{-3}$, where the right relic density requires $\Delta_h = 6(8) \times 10^{-4}$, i.e., it can introduce a tuning of $\mathcal{O}(0.01\%)$.

3. Type-III samples and Type-IV samples: $m_{\tilde{\chi}_1^0} \in (-800, -100) \text{GeV} \cup (100, 550) \text{GeV}$, $5 < \tan\beta < 60$, $300 \text{GeV} < \mu < 1000 \text{GeV}$, $100 \text{GeV} < M_2 < 1420 \text{GeV}$, and $\tilde{\chi}_1^0$ are mainly co-annihilated with wino-dominated electroweakinos ($\tilde{\chi}_2^0$ or $\tilde{\chi}_1^\pm$) (Type-III samples) or sleptons ($\tilde{\mu}_L$ or $\tilde{\mu}_R$) (Type-IV samples) to achieve the measured density. Here, we use $\Delta_{M_2} = (M_2 - |m_{\tilde{\chi}_1^0}|)/|m_{\tilde{\chi}_1^0}|$, and $\Delta_{m_i} = (M_{\tilde{\mu}_L \text{ or } \tilde{\mu}_R} - |m_{\tilde{\chi}_1^0}|)/|m_{\tilde{\chi}_1^0}|$ parameterizes the mass splitting between $\tilde{\chi}_1^0$ and wino-dominated electroweakinos or sleptons. From Fig. 2, we can conclude that

- the cases with $-400\text{GeV} < m_{\tilde{\chi}_1^0} < -100\text{GeV}$ have the "generalized blind spot", so $\sigma_{\tilde{\chi}_1^0-p}^{SI}$ can be small for small μ . However, the latest LZ experiment requires $\mu > 380\text{GeV}$. The observed relic density is obtained for mass splitting to parameterize $|\Delta_{M_2}| < 0.13$ or $|\Delta_{m_{\tilde{t}}}| < 0.18$.
- for the samples with $100\text{GeV} < m_{\tilde{\chi}_1^0} < 550\text{GeV}$, the contributions from h and H on $\sigma_{\tilde{\chi}_1^0-p}^{SI}$ reinforce each other, so $\sigma_{\tilde{\chi}_1^0-p}^{SI}$ is relatively large, and the latest LZ experiment has raised μ to above 600 GeV , which corresponds to $\Delta_{EW}^{-1} = 1\%$. The observed relic density is obtained for mass splitting to parameterize $|\Delta_{M_2}| < 0.07$ or $|\Delta_{m_{\tilde{t}}}| < 0.07$.
- for the region with $-800\text{GeV} < m_{\tilde{\chi}_1^0} < -400\text{GeV}$, although M_1/μ and $\tan\beta$ have opposite signs, the values of $|\mathcal{A}_h|$ are too large, so $\sigma_{\tilde{\chi}_1^0-p}^{SI}$ remains large for large μ . The latest LZ experiment has also increased μ to above 600 GeV , and the observed relic density is obtained for mass splitting parameterizes $|\Delta_{M_2}| < 0.07$ or $|\Delta_{m_{\tilde{t}}}| < 0.07$. In short, the characteristics of this area are similar to the cases with $100\text{GeV} < m_{\tilde{\chi}_1^0} < 550\text{GeV}$. Moreover, these regions of the parameter space will shrink or disappear with further improvement of sensitivity in future experiments.

From the above analysis, considering the latest dark matter experimental results, the MSSM becomes very unnatural to simultaneously explain the dark matter scattering cross section and residual density. This situation will be further exacerbated if future DM DD experiments fail to detect the signs of DM. On further considering other experimental limitations such as the rapid progress of the LHC search for supersymmetry[17, 11, 18] and recent measurement of muon anomalous magnetic moment at Fermilab [15], as shown in Ref. [14], the surviving region greatly decreases, and the lower boundary of μ further increases, which imply that the MSSM is even more unnatural.

4 Conclusion

The LZ experiment recently released its first results in the direct search for DM, where the sensitivities to the spin-independent (SI) and spin-dependent (SD) cross sections of DM-nucleon scattering have reached approximately $6.0 \times 10^{-48} \text{ cm}^2$ and $1.0 \times 10^{-42} \text{ cm}^2$, respectively, for the DM mass of approximately 30 GeV [16]. These unprecedented precision values strongly limit the DM coupling to the SM particles, which are determined by SUSY parameters. Faced with this strong experimental limitation, the DM phenomenology and unnaturalness related to DM physics in the MSSM are discussed in detail using approximate analytical formulas. The study found that under the limit of the latest dark matter experiment, the unnaturalness associated with DM in the MSSM is embodied in the large higgsino mass (μ) raised by the latest LZ experiment requirement. For example, if the Z - or h -mediated resonant annihilations should achieve the measured dark matter density, the LZ experiment requires a larger μ than approximately 500 GeV or TeV in magnitude. These improved bounds imply a tuning to predict the Z -boson mass and simultaneously worsen the naturalness of the Z - and h -mediated resonant annihilations to achieve the measured dark matter density.

Acknowledgments

We sincerely thank Prof. Junjie Cao for numerous helpful discussions and his great effort to improve the manuscript. We thank LetPub for its linguistic assistance during the preparation of this manuscript.

References

- [1] S. P. Martin, In *Perspectives on supersymmetry II*, edited by G. L. Kane: 1-153 [hep-ph/9709356].
- [2] G. Aad *et al.* [ATLAS Collaboration], *Phys. Lett. B* **716** (2012) 1.
- [3] S. Chatrchyan *et al.* [CMS Collaboration], *Phys. Lett. B* **716** (2012) 30.
- [4] See *e.g.* M. Shifman, *Mod. Phys. Lett. A* **27** (2012) 1230043.
- [5] H. Baer and X. Tata, *Weak Scale Supersymmetry: From Superfields to Scattering Events*, (Cambridge University Press, 2006).
- [6] H. Baer, V. Barger, P. Huang, A. Mustafayev and X. Tata, *Phys. Rev. Lett.* **109** (2012) 161802; H. Baer, V. Barger, P. Huang, D. Mickelson, A. Mustafayev and X. Tata, arXiv:1212.2655 [hep-ph].
- [7] H. Baer, V. Barger and M. Padeffke-Kirkland, *Phys. Rev. D* **88** (2013), 055026 doi:10.1103/PhysRevD.88.055026 [arXiv:1304.6732 [hep-ph]].
- [8] E. Bagnaschi, K. Sakurai, M. Borsato, O. Buchmueller, M. Citron, J. C. Costa, A. De Roeck, M. J. Dolan, J. R. Ellis and H. Flächer, *et al.* *Eur. Phys. J. C* **78** (2018) no.3, 256 doi:10.1140/epjc/s10052-018-5697-0 [arXiv:1710.11091 [hep-ph]].
- [9] X. Cui *et al.* [PandaX-II], *Phys. Rev. Lett.* **119** (2017) no.18, 181302 doi:10.1103/PhysRevLett.119.181302 [arXiv:1708.06917 [astro-ph.CO]].
- [10] C. Amole *et al.* [PICO], *Phys. Rev. Lett.* **118** (2017) no.25, 251301 doi:10.1103/PhysRevLett.118.251301 [arXiv:1702.07666 [astro-ph.CO]].
- [11] A. M. Sirunyan *et al.* [CMS], *JHEP* **03** (2018), 160 doi:10.1007/JHEP03(2018)160 [arXiv:1801.03957 [hep-ex]].
- [12] M. Drees and G. Ghaffari, *Phys. Rev. D* **104** (2021) no.7, 075031 doi:10.1103/PhysRevD.104.075031 [arXiv:2103.15617 [hep-ph]].
- [13] E. Aprile *et al.* [XENON], *Phys. Rev. Lett.* **121** (2018) 111302, doi:10.1103/PhysRevLett.121.111302 [arXiv:1805.12562 [astro-ph.CO]].
- [14] Y. He, L. Meng, Y. Yue and D. Zhang, [arXiv:2303.02360 [hep-ph]].
- [15] MUON G-2 collaboration, B. Abi *et al.*, *Phys. Rev. Lett.* **126** (2021) 141801.
- [16] LZ collaboration, J. Aalbers *et al.*, 2207.03764.

- [17] ATLAS collaboration, G. Aad et al., *Eur. Phys. J. C* **81** (2021) 1118.
- [18] CMS collaboration, A. M. Sirunyan et al., *JHEP* **03** (2018) 166
- [19] A. Pierce, N. R. Shah and K. Freese, [arXiv:1309.7351 [hep-ph]].
- [20] H. E. Haber and G. L. Kane. *Phys. Rept.* **117** (1985) 75.
- [21] J.F. Gunion and H.E. Haber. *Nucl. Phys. B* **272** (1986) 1[Nuclear Physics B 402.1-2(1993):569].
- [22] S. Baum, M. Carena, N. R. Shah, and C. E. M. Wagner, *JHEP* **01** (2022) 025.
- [23] S. Baum, M. Carena, T. Ou, D. Rocha, N. R. Shah and C. E. M. Wagner, *JHEP* **11** (2023), 037 doi:10.1007/JHEP11(2023)037 [arXiv:2303.01523 [hep-ph]].
- [24] M. Badziak, M. Olechowski and P. Szczerbiak, *JHEP* **1603**, 179 (2016) doi:10.1007/JHEP03(2016)179 [arXiv:1512.02472 [hep-ph]].
- [25] M. Badziak, M. Olechowski and P. Szczerbiak, *JHEP* **1707**, 050 (2017) doi:10.1007/JHEP07(2017)050 [arXiv:1705.00227 [hep-ph]].
- [26] M. Drees and M. M. Nojiri, *Phys. Rev. D* **48**, 3483 (1993) doi:10.1103/PhysRevD.48.3483 [hep-ph/9307208].
- [27] M. Drees and M. M. Nojiri, *Phys. Rev. D* **47**, 4226 (1993) doi:10.1103/PhysRevD.47.4226 [hep-ph/9210272].
- [28] G. Belanger, F. Boudjema, A. Pukhov and A. Semenov, *Comput. Phys. Commun.* **180**, 747 (2009) doi:10.1016/j.cpc.2008.11.019 [arXiv:0803.2360 [hep-ph]].
- [29] Q. Riffard, F. Mayet, G. Bélanger, M.-H. Genest and D. Santos, *Phys. Rev. D* **93**, no. 3, 035022 (2016) doi:10.1103/PhysRevD.93.035022 [arXiv:1602.01030 [hep-ph]].
- [30] P. Huang and C. E. M. Wagner, “Blind Spots for neutralino Dark Matter in the MSSM with an intermediate m_A ,” *Phys. Rev. D* **90**, 015018(2014).
- [31] **Planck** Collaboration, N. Aghanim *et al.*, “Planck 2018 results. VI. Cosmological parameters,” *Astron. Astrophys.* **641** (2020) A6 [Erratum: *Astron. Astrophys.* 652, C4 (2021)].
- [32] J. Cao, L. Meng, Y. Yue, H. Zhou and P. Zhu, *Phys. Rev. D* **101** (2020) no.7, 075003 doi:10.1103/PhysRevD.101.075003 [arXiv:1910.14317 [hep-ph]].
- [33] T. Han, Z. Liu, and A. Natarajan, “Dark matter and Higgs bosons in the MSSM, *JHEP* **11** (2013) 008.
- [34] M. E. Cabrera, J. A. Casas, A. Delgado, *et al.*, “Naturalness of MSSM dark matter, *JHEP* **08** (2016) 058.
- [35] S. Baum, M. Carena, N. R. Shah and C. E. M. Wagner, *JHEP* **04** (2018), 069 doi:10.1007/JHEP04(2018)069 [arXiv:1712.09873 [hep-ph]].
- [36] K. Griest and D. Seckel, *Phys. Rev. D* **43**, 3191 (1991). doi:10.1103/PhysRevD.43.3191

- [37] J. R. Ellis, T. Falk, and K. A. Olive, “Neutralino - Stau coannihilation and the cosmological upper limit on the mass of the lightest supersymmetric particle, *Phys. Lett. B* **444** (1998) 367–372
- [38] J. R. Ellis, T. Falk, K. A. Olive, and M. Srednicki, “Calculations of neutralino-stau coannihilation channels and the cosmologically relevant region of MSSM parameter space,” *Astropart. Phys.* **13** (2000) 181–213, [Erratum: *Astropart. Phys.* 15, 413–414 (2001)].
- [39] M. R. Buckley, D. Hooper, and J. Kumar, “Phenomenology of Dirac Neutralino Dark Matter, *Phys. Rev. D* **88** (2013) 063532,
- [40] M. J. Baker and A. Thamm, “Leptonic WIMP Coannihilation and the Current Dark Matter Search Strategy,” *JHEP* **10** (2018) 187,
- [41] T. T. Yanagida, W. Yin, and N. Yokozaki, “Bino-wino coannihilation as a prediction in the E_7 unification of families,” *JHEP* **12** (2019) 169,
- [42] F. Feroz, M. P. Hobson and M. Bridges, *MultiNest: an efficient and robust Bayesian inference tool for cosmology and particle physics*, *Mon. Not. Roy. Astron. Soc.* **398** (2009) 1601.
- [43] P. Bechtle, S. Heinemeyer, T. Klingl, T. Stefaniak, G. Weiglein and J. Wittbrodt, *HiggsSignals-2: Probing new physics with precision Higgs measurements in the LHC 13 TeV era*, *Eur. Phys. J. C* **81** (2021) 145.
- [44] P. Bechtle, D. Dercks, S. Heinemeyer, T. Klingl, T. Stefaniak, G. Weiglein et al., *HiggsBounds-5: Testing Higgs Sectors in the LHC 13 TeV Era*, *Eur. Phys. J. C* **80** (2020) 1211.
- [45] PANDAX-4T collaboration, Y. Meng et al., *Dark Matter Search Results from the PandaX-4T Commissioning Run*, *Phys. Rev. Lett.* **127** (2021) 261802.
- [46] XENON collaboration, E. Aprile et al., *Constraining the spin-dependent WIMP-nucleon cross sections with XENON1T*, *Phys. Rev. Lett.* **122** (2019) 141301.
- [47] PARTICLE DATA GROUP collaboration, M. Tanabashi, K. Hagiwara, Hikasa et al., *Phys. Rev. D* **98** (2018) 030001.
- [48] J. E. Camargo-Molina, B. O’Leary, W. Porod and F. Staub, *Vevacious: A Tool For Finding The Global Minima Of One-Loop Effective Potentials With Many Scalars*, *Eur. Phys. J. C* **73** (2013) 2588.
- [49] J. E. Camargo-Molina, B. Garbrecht, B. O’Leary, W. Porod and F. Staub, *Constraining the Natural MSSM through tunneling to color-breaking vacua at zero and non-zero temperature*, *Phys. Lett. B* **737** (2014) 156.